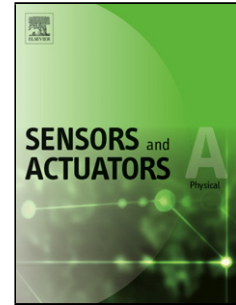


## Accepted Manuscript

Title: A simple load sensor based on a bent single-mode–multimode–single-mode fiber structure

Author: A.Z. Zulkifli S.E.F. Masnan N.M. Azmi S.M. Akib  
H. Arof S.W. Harun



PII: S0924-4247(16)30079-6  
DOI: <http://dx.doi.org/doi:10.1016/j.sna.2016.02.025>  
Reference: SNA 9536

To appear in: *Sensors and Actuators A*

Received date: 11-10-2015  
Revised date: 11-2-2016  
Accepted date: 12-2-2016

Please cite this article as: A.Z.Zulkifli, S.E.F.Masnan, N.M.Azmi, S.M.Akib, H.Arof, S.W.Harun, A simple load sensor based on a bent single-modendashmultimodendashsingle-mode fiber structure, Sensors and Actuators: A Physical <http://dx.doi.org/10.1016/j.sna.2016.02.025>

This is a PDF file of an unedited manuscript that has been accepted for publication. As a service to our customers we are providing this early version of the manuscript. The manuscript will undergo copyediting, typesetting, and review of the resulting proof before it is published in its final form. Please note that during the production process errors may be discovered which could affect the content, and all legal disclaimers that apply to the journal pertain.

# A simple load sensor based on a bent single-mode-multimode-single-mode fiber structure

A. Z. Zulkifli<sup>1</sup>, S. E. F. Masnan<sup>2</sup>, N. M. Azmi<sup>2</sup>, S. M. Akib<sup>3</sup>, H. Arof<sup>1</sup> and S. W. Harun<sup>1</sup>

<sup>1</sup>Department of Electrical Engineering, University of Malaya, 50603 Kuala Lumpur, Malaysia

<sup>2</sup>Department of Civil Engineering, University of Malaya, 50603 Kuala Lumpur, Malaysia

<sup>3</sup>School of Energy, Geoscience, Infrastructure and Society (EGIS), Heriot-Watt University Malaysia, No. 1 Jalan Venna P5/2, Precinct 5, 62200 Putrajaya, Malaysia.

Email: swharun@um.edu.my

## Highlights

- A load sensor uses a single-mode-multimode-single-mode (SMS) fiber structure.
- The SMS structure is sandwiched between two CR-39 plastic polymer plates.
- A larger effective transverse strain can be achieved when the distance between the stage and the edge of the multimode fiber is larger.
- The SMS device is suitable for sensing a small load or transverse strain with a reasonably high sensitivity.

## Abstract

A load sensor is demonstrated using a single-mode-multimode-single-mode (SMS) fiber structure, which is sandwiched between two CR-39 plastic polymer plates. A larger effective transverse strain can be achieved when the distance,  $D_2$ , between the stage and the edge of the multimode fiber is larger. A higher sensitivity is obtained when  $D_2 = 7$  cm with a value of  $-0.0102$  nm/mN, as compared to  $-0.0027$  nm/mN when  $D_2 = 3$  cm. In contrast, an FBG integrated in a similar manner has shown an indiscernible change in the wavelength shift as compared to that produced by the SMS device. The result indicates that the proposed SMS device is suitable for sensing a small load or transverse strain with a reasonably high sensitivity.

1

2 **Keywords:** interferometer, load sensor, fiber-optic sensor.

3

4

5

## 6 **Introduction**

7         Optical fiber sensors have been widely used in measuring various physical, chemical,  
8 and even biological parameters, as they are compact, responsive, sensitive, stable and resistant  
9 to electromagnetic interference [1-2]. They have also been recommended for applications in  
10 areas such as structural monitoring of buildings [3], estimation of metal surface roughness [4],  
11 vibration tests [5], determination of the thickness of a transparent plate [6], etc. A fiber Bragg  
12 grating (FBG) based optical sensor is widely used and by far is the most common type of fiber  
13 sensors [7-8]. However, it suffers from a narrow measurement range especially when used for  
14 strain sensing, and consequently requires a mechanical arrangement to improve the  
15 measurement range and a complex interrogation system to achieve a high wavelength  
16 resolution. A single mode–multimode–single mode (SMS) fiber structure has also been  
17 proposed as a strain sensor as it generates a sufficient bandpass spectral response for a given  
18 wavelength range [9-10]. It can be used as either a stand-alone sensor or an edge filter that  
19 interrogates an optical sensor such as an FBG. Since an SMS fiber structure is much easier to  
20 fabricate than an FBG, a sensor based on an SMS fiber structure will be more economic than  
21 the one based on an FBG. In the past, the SMS fiber based sensor has been exploited in various  
22 applications such as displacement [11], pressure [12] and temperature sensors [13-14].

23         A straight SMS fiber structure can be used as a load sensor, but just like an FBG sensor,  
24 a straight SMS structure suffers from a narrow measurement range, due to the limited strain  
25 that can be applied to avoid breaking it. In this paper, we propose to use a bent SMS fiber

1 structure to measure load or strain. This technique offers the advantages of a much simpler  
2 configuration, ease of fabrication, wide strain measurement range up to 2800  $\mu\epsilon$  [15] and high  
3 resolution.

4

### 5 **Experimental arrangement**

6 In recent years, in-line fiber-optic Fabry-Perot interferometers (FPIs) have received  
7 much attention for a wide range of applications. Fabricating an in-line fiber optic FPI requires  
8 the formation of two parallel separated mirrors to partially reflect the input optical signals into  
9 different optical paths. Numerous techniques have been employed to form the mirrors in the  
10 SMF, such as coating the end of the fiber [16], using offset structures [17], forming a micro-  
11 notch by use of femtosecond lasers [18], using chemical etching [19], splicing [20], etc. Since  
12 the two beams reflected by the mirrors have an optical path difference (OPD), the relative phase  
13 difference of the two beams could be described by:

$$14 \quad \phi_{FPI} = \frac{4\pi nL}{\lambda} \quad (1)$$

15 where  $\lambda$  is the input wavelength,  $n$  is the refractive index (RI) of FPI cavity, and  $L$  is the length  
16 of the FPI cavity. When a perturbation is applied to the FPI, the phase difference  $\phi_{FPI}$  between  
17 the two beams will be influenced because the cavity length increases. The change of  $\phi_{FPI}$   
18 contributes to the interference shifts, which allows the FPI to be used for temperature or strain  
19 sensing.

20

21

22

23

1

2

3

4

5

6

7

8

9

10

11

12

13

14

15

16

17

18

19

20

21

22

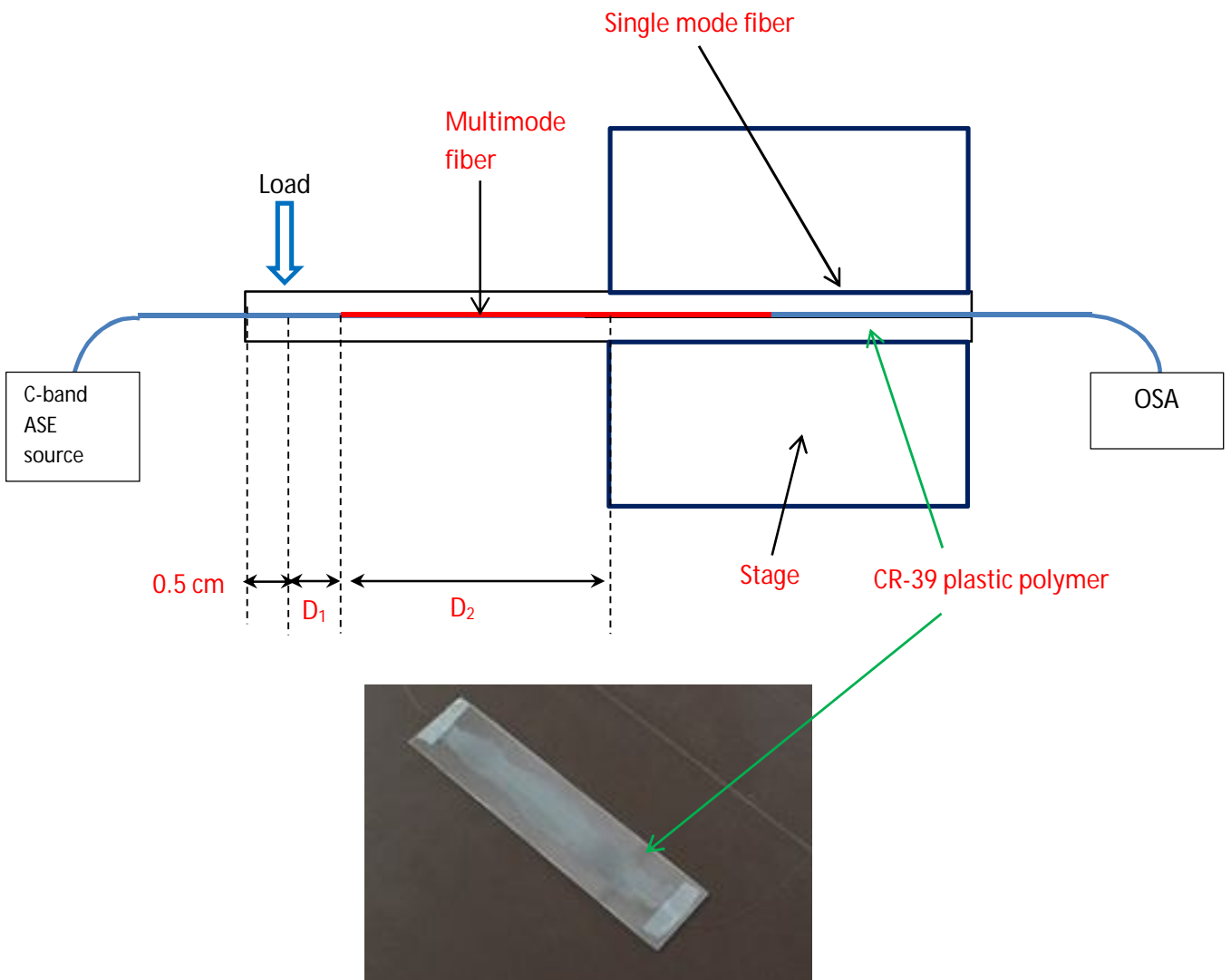
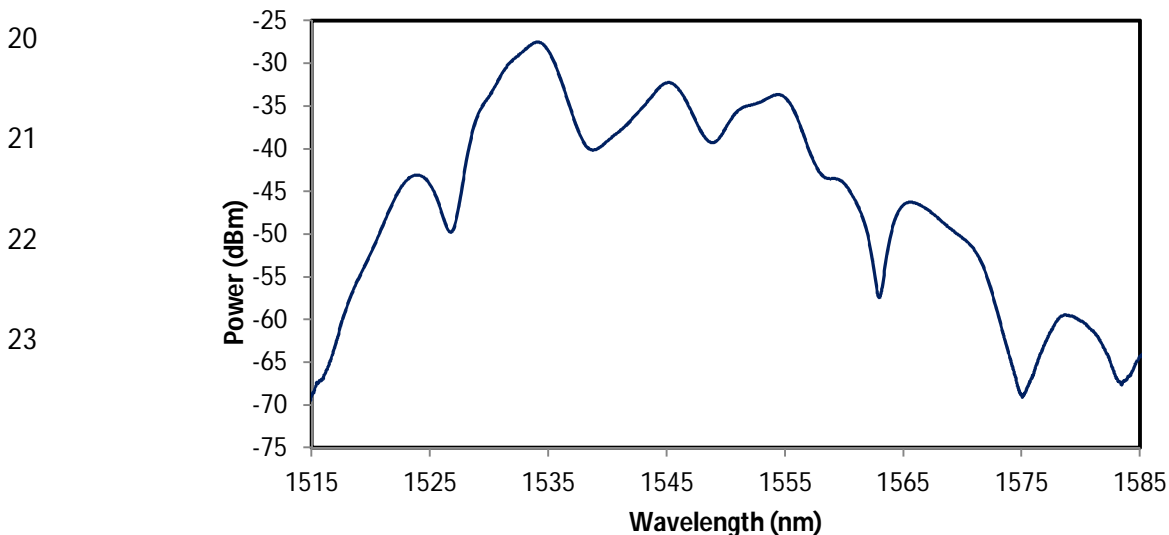


Fig. 1: Schematic diagram of the proposed load sensor experimental setup utilizing an SMS fiber structure. Inset shows the photo-image of the SMS structure.

1 In this work, we propose a specially designed SMS fiber structure as an FPI sensor. Fig.  
 2 1 shows a schematic diagram of a straight SMS fiber structure, which is sandwiched between  
 3 two CR-39 plastic polymer plates with a thickness of 0.05 cm, width of 4 cm and length of 17.4  
 4 cm. Epoxy is used to integrate the device. The MMF has a step-index profile with a core  
 5 diameter of 50  $\mu\text{m}$  and length of 9.3 cm. It is fusion spliced with the single mode fiber (SMF-  
 6 28) with a splicing loss of less than 0.1 dB to form the SMS structure. The device is clamped  
 7 between two stages as shown where the distance between the stage and multimode input  
 8 endpoint is labelled as  $D_2$ . It is noted that, the edge of the clamping stage is set within the  
 9 multimode fiber region as shown in the schematic.

10 Light from an Erbium amplified spontaneous emission (ASE) source centered around  
 11 1550 nm is launched into the SMS structure. The light injected into the MMF from a SMF will  
 12 excite multiple modes propagating in the MMF. The output spectrum measured at room  
 13 temperature using an optical spectrum analyser (OSA) at a resolution of 0.05 nm is shown in  
 14 Fig. 2, at zero loading and  $D_2 = 7$  cm. For a straight fiber, the refractive index along the  
 15 propagation direction is symmetrically distributed. The SMS fiber structure has a bandpass  
 16 spectral response for the wavelength range shown in Fig. 2. The bandpass response is a result  
 17 of multimode interference and recoupling within the SMS fiber structure. As observed, the  
 18 comb spectrum obtained has a fixed peak to peak spacing of about 11 nm. The interference  
 19 spectrum changes when strain is applied on the multimode fiber.



1

2

3

Fig. 2: Output spectrum from a straight SMS fiber structure.

4

## 5 **Result and discussion**

6

7 In order to investigate the effect of transverse load on the SMS structure, a loading  
8 fixture is used as shown in Fig. 1. This fixture is designed to create a uniform state of plane  
9 strain on the fiber core in the vicinity of the MMF. Load is applied to the structure by hanging  
10 weights at the end of a load arm with  $D_1 = 4.5$  cm. The test procedure for the experiments is as  
11 follows. The SMS structure is placed in the fixture with  $D_2 = 7$  cm, and measurements of the  
12 wavelengths of the interference peaks are taken for unloaded condition. The load on the fiber  
13 is then incrementally increased up to 262.8 mN and the center wavelengths of the interference  
14 peaks are recorded at each load value. The fiber is then unloaded and the tests are repeated at  
15  $D_2 = 3$  cm. When transverse strain or load is applied to a straight SMS fiber structure, the MMF  
16 length changes causing the phase differences between these multiple modes and subsequently  
17 the spectral response of the structure to change as well. The measured spectral response of the  
18 SMS fiber structure at  $D_2 = 7$  cm and  $D_2 = 3$  cm are shown in Figs. 3 and 4 respectively, for  
19 various values of transverse strain or loads. In the experiment, the measurements were taken at  
20 a span of 20 nm and resolution of 0.05 nm. As shown in both figures, both peak wavelength  
21 and bandwidth of the interference comb change as the load increases.

21

22

1

2

3

4

5

6

7

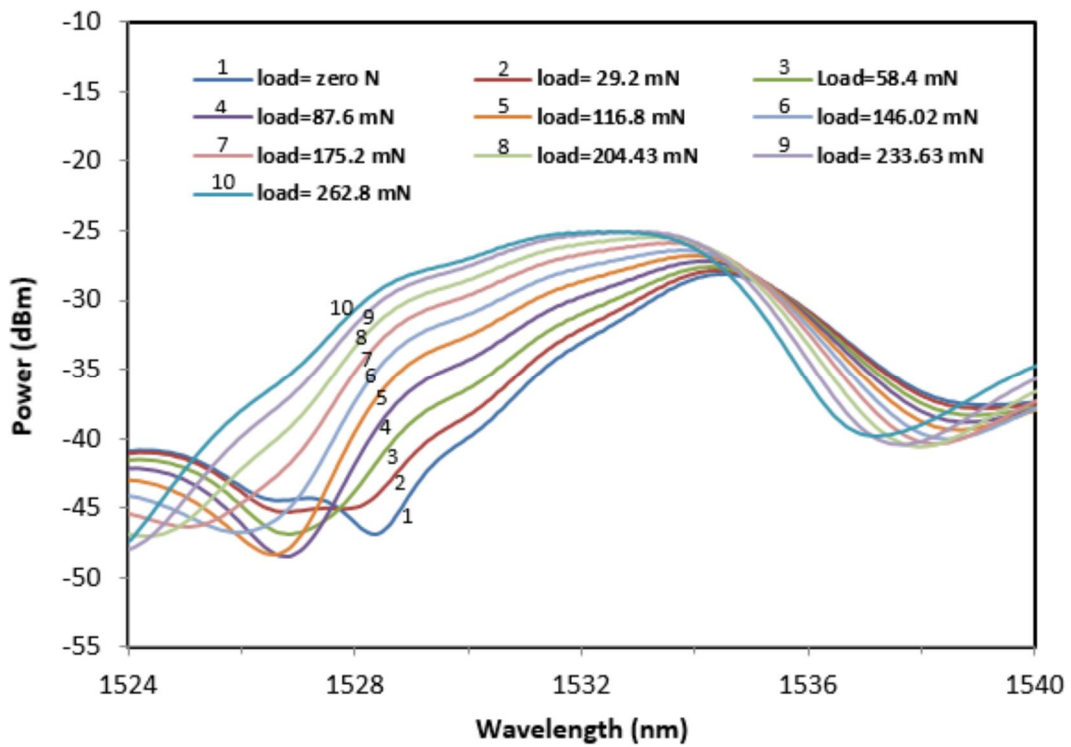
8

9

10

11

12

13 Fig. 3: The measured spectral response from the SMS structure at different load values at  $D_2$ 

14

= 7 cm

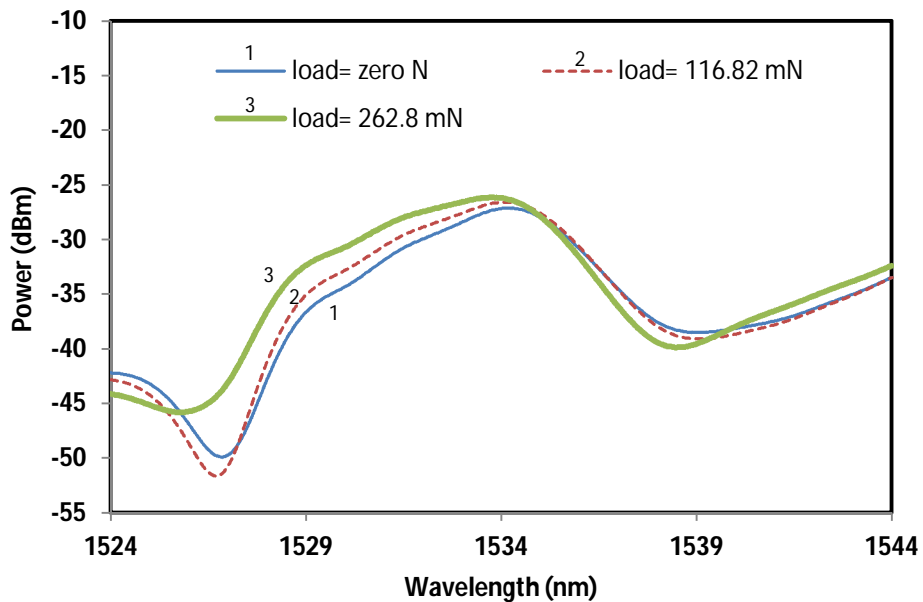
15

16

17

18

19



1

2

3 Fig. 4: The measured spectral response from the SMS structure at different load values at  $D_2$ 4  $= 3 \text{ cm}$ 

5 For a bent MMF, the refractive index distribution is no longer symmetric and must be

6 defined by an equivalent refractive index distribution as follows [21]:

7 
$$n = n_0 \left( 1 + \frac{x}{R_{eff}} \right), \quad (2)$$

8 where  $n_0(x, y)$  is the refractive index of the straight fiber and  $R_{eff}$  is the equivalent bent radius

9 which can be expressed as follows [21]:

10 
$$R_{eff} = \frac{R}{1 - \frac{n_0^2}{2}[P_{12} - \nu(P_{12} + P_{12})]}, \quad (3)$$

11 where  $R$  is the bent radius of the fiber,  $\nu$  is the Poisson ratio and  $P_{11}$  and  $P_{12}$  are components of

12 the photo-elastic tensor. Eq. (3) shows that the field distribution in the bent MMF portion is

13 asymmetric since the bent MMF effectively has an asymmetric refractive index distribution as

14 illustrated in Eq. (2). The bend in the MMF section has a significant influence on the mode

15 distribution in the SMS fiber structure, which in turn will have a profound effect on the overall

16 transmission characteristics of the SMS structure as shown in Figs. 3 and 4. It can be inferred

17 from both figures that the peak 3dB bandwidth increases while the peak wavelength of the

18 interference comb spectrum shifts to a shorter wavelength as the load grows. In addition the

19 peak power also increases with load increment.

20 The relation between the peak of interference wavelength and the amount of load at two

21 different  $D_2$  distances is illustrated in Fig. 5. As shown in the figure, the peak wavelength

22 linearly shifts to a shorter wavelength with load increment. The slopes of the variation are

1 obtained at  $-0.0102 \text{ nm / mN}$  and  $-0.0027 \text{ nm/mN}$  for  $D_2 = 7 \text{ cm}$  and  $D_2 = 3 \text{ cm}$ , respectively.

2 This shows that the sensor sensitivity increases as the distance between the load and the edge

3 of the clamped stage increases. The lower slope achieved when  $D_2 = 3 \text{ cm}$ , shows that the

4 effective transverse strain applied on MMF is smaller compared to when  $D_2 = 7 \text{ cm}$ . This is

5 attributed to the increased in the equivalent bending radius, which in turn changes the mode

6 distribution, phase shift and reduces the equivalent refractive index of the MMF as indicated

7 in Eqs. 3, 2 and 1, respectively. Hence, smaller change of MMF equivalent refractive index is

8 achieved when  $D_2 = 3 \text{ cm}$  which leads to lower sensitivity. The 3 dB bandwidth of the output

9 spectral against the load at two different  $D_2$  distances is shown in Fig. 6 where the 3 dB

10 bandwidth increases linearly with the load for both curves. The slopes of the graph are  $0.0085$

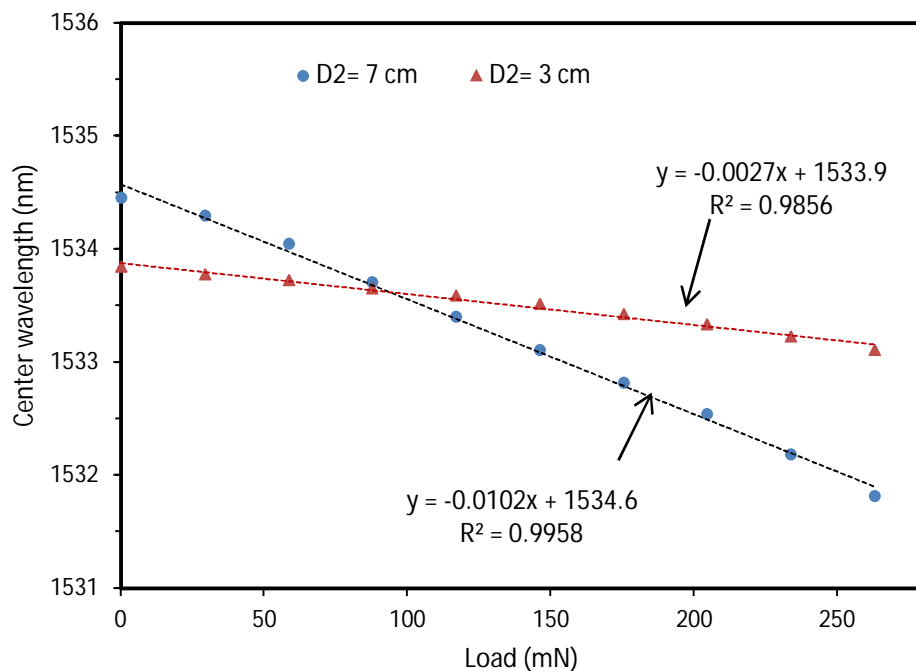
11  $\text{nm/mN}$  and  $0.0024 \text{ nm/mN}$  for  $D_2 = 7 \text{ cm}$  and  $3 \text{ cm}$  respectively. The 3 dB bandwidth change

12 is more pronounced for higher  $D_2$  due to the increased phase shift. The highest value of  $D_2$  is

13 limited by the length of the plastic polymer in conjunction with how much it can securely clamp

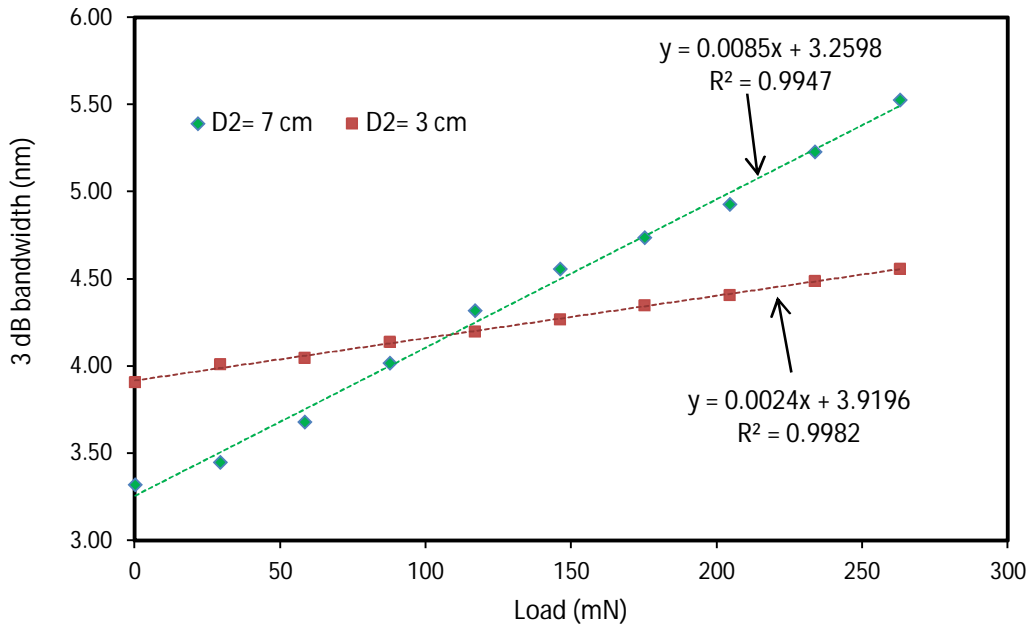
14 to the stage as shown in Fig. 1. To securely clamp the plastic polymer plate, it is advice that at

15 least half of the stage distance is clamping the plate



16  
17  
18  
19  
20  
21  
22  
23  
24  
25  
26

1 Fig 5: Central peak wavelength of the interference spectrum against the amount of load for  
 2 two different  $D_2$  values.



3  
 4 Fig 6: 3 dB bandwidth of the interference spectrum against the amount of load for two  
 5 different  $D_2$  values.

6  
 7 A similar test on an FBG based sensor using the same setup as shown in Fig 1 is  
 8 performed for comparison purpose. The FBG is placed between the same CR-39 plastic  
 9 polymer plates of the same dimension. However, the edge of the stage is fixed at the center of  
 10 the FBG, with  $D_2 = 7$  cm,  $D_1 = 4.5$  cm (the center point of load to the edge of the FBG). The  
 11 FBG has a bandwidth of 0.173 nm, length of 2 cm, and reflectivity of 99.97 %. Fig 7 shows  
 12 the output transmission spectrum measured using OSA at the smallest span setting of 0.5 nm  
 13 and resolution of 0.05 nm at different loads. It can be inferred that there is hardly any change  
 14 in the center wavelength even when load of 262.8 mN is applied.

15  
 16  
 17

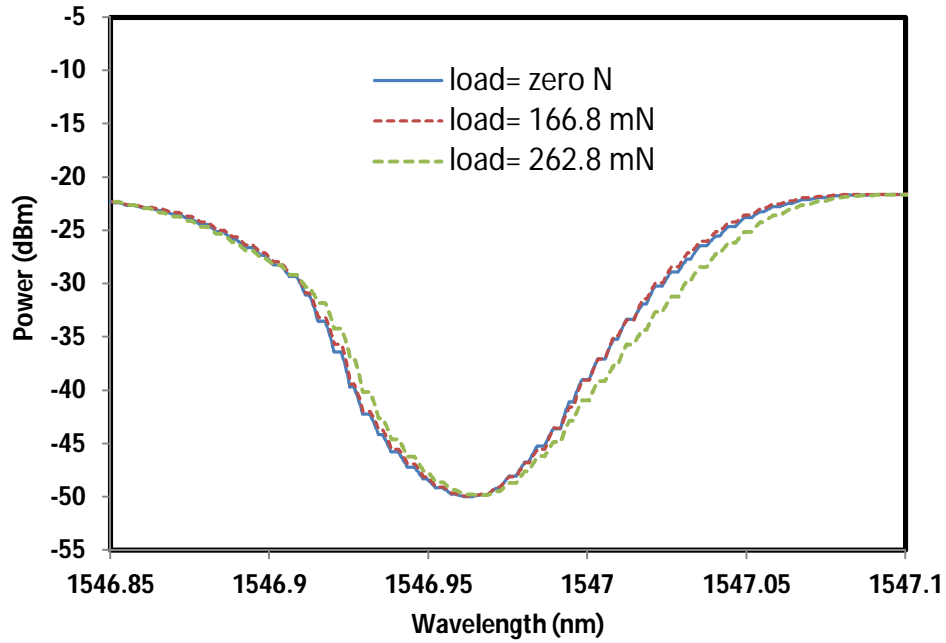


Fig 7: Transmission spectrum of the FBG based sensor at different loads

A center wavelength of 1546.961 nm and 1546.966 nm are observed at zero load and 262.8 mN load respectively. This gives a wavelength shift of merely 0.005 nm at maximum load. This change of wavelength is too small for practical load sensing since the signal can be corrupted by noise from the instability of ASE source and ambient temperature. In contrast, for the SMS structure, at  $D_2 = 7$  cm, the wavelength shift of 2.64 nm is obtained at maximum load. This shows that the SMS device has a higher sensitivity than the FBG.

## Conclusion

In this paper, the performance of a load sensor that uses an SMS fiber structure integrated between two plates of CR-39 plastic polymer and clamped onto a stage is evaluated. It is found that, a larger effective transverse strain can be obtained when the distance,  $D_2$  between the edge of the multimode fiber and the edge of the stage is larger. A slope of -0.0102 nm/mN and -

1 0.0027 nm/mN are obtained for  $D_2= 7$  cm and 3 cm respectively; where higher sensitivity is  
2 achieved when  $D_2= 7$ cm. Moreover, it is found that an FBG sensor integrated and tested in a  
3 similar manner shows lower sensitivity. In short, the SMS device is shown to be a better load  
4 sensor where small load or strain is concerned.

5

## 6 **Acknowledgment**

7 This work is financially supported by Ministry of Higher Education under High Impact  
8 Research Grant Scheme (Grant No: UM.C/625/1/HIR/MOHE/ENG/61)

9

## 10 **References**

- 11 1. H. A Rahman, H. R. A Rahim, H. Ahmad, M. Yasin, R. Apsari, S. W. Harun, "Fiber optic  
12 displacement sensor for imaging of tooth surface roughness," *Measurement* 46 (1), pp. 546-  
13 551 (2013)
- 14 2. M. S. Ferreira, M. Becker, H. Bartelt, P. Mergo, J. L. Santos and O. Frazão, "A vibration  
15 sensor based on a distributed Bragg reflector fibre laser," *Laser Physics Letters*, vol. 10(9),  
16 pp. 095102 (2013).
- 17 3. N. Metje, D. N. Chapman, C. D. F. Rogers, P. Henderson and M. Beth, "An optical fiber  
18 sensor system for remote displacement monitoring of structures—prototype tests in the  
19 laboratory," *Struct. Health Monit.*, vol. 7, pp. 51–63 (2008).
- 20 4. S. W. Harun, M. Yasin, H. Z. Yang, H Z, Kusminarto, Karyono and H. Ahmad, "Estimation  
21 of metal surface roughness using fiber optic displacement sensor," *Laser Phys.*, vol. 20, pp.  
22 904–909 (2010)

- 1 5. A. Vallan, M. L. Casalicchio and G. Perrone, "Displacement and acceleration  
2 measurements in vibration tests using a fiber optic sensor," *IEEE Trans. Instrum. Meas.*,  
3 vol. 59, pp. 1389–96 (2010).
- 4 6. D. Sastikumar, G. Gobi and B. Renganathan, "Determination of the thickness of a  
5 transparent plate using a reflective fiber optic displacement sensor," *Opt. Laser Technol.*,  
6 vol. 42, pp. 911–917 (2010).
- 7 7. Q. Wu, Y. Semenova, A. Sun, P. Wang and G. Farrell, "High resolution temperature  
8 insensitive interrogation technique for FBG sensors," *Opt. Laser Technol.*, vol. 42, pp. 653–  
9 656, (2010).
- 10 8. S. O. Park, B. W. Jang, Y. G. Lee, C. G. Kim and C. Y. Park, "Simultaneous measurement  
11 of strain and temperature using a reverse index fiber Bragg grating sensor," *Meas. Sci.*  
12 *Technol.*, vol. 21, pp. 035703 (2010)
- 13 9. D. P. Zhou, L. Wei, W. K. Liu and J. W. Y. Lit, "Simultaneous strain and temperature  
14 measurement with fiber Bragg grating and multimode fibers using an intensity-based  
15 interrogation method," *IEEE Photonics Technol. Lett.*, vol. 21, pp. 468–470 (2008)
- 16 10. Q. Wu, A. M. Hatta, Y. Semenova and G. Farrell, "Use of a SMS fiber filter for  
17 interrogating FBG strain sensors with dynamic temperature compensation," *Appl. Opt.*,  
18 vol. 48, pp. 5451–5458 (2009)
- 19 11. Q. Wu, A. M. Hatta, P. Wang, Y. Semenova and G. Farrell, "Use of a Bent Single SMS  
20 Fiber Structure for Simultaneous Measurement of Displacement and Temperature  
21 Sensing." *IEEE Photon. Technol. Lett.*, vol. 23, pp. 130 - 132 (2011)
- 22 12. V. I. Ruiz-Pérez, M. A. Basurto-Pensado, P. LiKamWa, J. J. Sánchez-Mondragón and D.  
23 A. May-Arriolja, (2011, January). "Fiber optic pressure sensor using multimode  
24 interference." *Journal of Physics: Conference Series*, vol. 274, pp. 012025 (2011).

- 1 13. R. X. Gao, Q. Wang, F. Zhao, B. Meng and S. L. Qu, “Optimal design and fabrication of  
2 SMS fiber temperature sensor for liquid,” Opt. Comm., vol. 283, pp. 3149-3152, (2010)
- 3 14. Q. Wu, Y. Semenova, A. M. Hatta, P. Wang and G. Farrell, “Bent SMS fibre structure for  
4 temperature measurement,” Electr. Let., vol. 46, pp. 1129-1130, (2010)
- 5 15. Y. Liu and L. Wei, “Low-cost high-sensitivity strain and temperature sensing using graded-  
6 index multimode fibers,” Appl. Opt., vol. 46, pp. 2516-2519, (2007).
- 7 16. J. R. Zhao, X. G. Huang, W. X. He, and J. H. Chen, “High-resolution and temperature-  
8 insensitive fiber optic refractive index sensor based on fresnel reflection modulated by  
9 Fabry-Perot interference,” J. Lightw. Technol., vol. 28, pp. 2799–2803, (2010).
- 10 17. D. W. Duan, Y. J. Rao, and T. Zhu, “High sensitivity gas refractometer based on all-fiber  
11 open-cavity Fabry-Perot interferometer formed by large lateral offset splicing,” JOSA B,  
12 vol. 29, pp. 912–915 (2012).
- 13 18. T. Wei, Y. K. Han, Y. J. Li, H. L. Tsai and H. Xiao, “Temperature-insensitive miniaturized  
14 fiber inline Fabry-Perot interferometer for highly sensitive refractive index measurement,”  
15 Opt. Express, vol. 16, pp. 5764–5769 (2008).
- 16 19. V. R. Machavaram, R. A. Badcock and G. F. Fernando, “Fabrication of intrinsic fibre  
17 Fabry-Perot sensors in silica fibres using hydrofluoric acid etching,” Sens. Actuat. A, vol.  
18 138, pp. 248–260 (2007)
- 19 20. D. W. Duan, Y. J. Rao, Y. S. Hou and T. Zhu, “Microbubble based fiber-optic Fabry-Perot  
20 interferometer formed by fusion splicing single-mode fibers for strain measurement,” Appl.  
21 Opt., vol. 51, pp. 1033–1036 (2012).
- 22 21. D. H. Kim, J. W. Park, H. K. Kang, C. S. Hong and C. G. Kim, “Measuring dynamic strain  
23 of structures using a gold-deposited extrinsic Fabry-Perot interferometer,” Smart Mater.  
24 Struct., vol. 12, pp. 1–5, (2003).

25 **22.**

26 **23.**



1 24.

2 25.

3 26.

4 27. **Ahmad Zarif Zulkifli** was born in Kuala Lumpur, Malaysia, in 1984. He received his  
 5 B.E. degree in electrical engineering from the University Teknologi Malaysia, Malaysia,  
 6 in 2008, and the M. Eng. Degree In Telecommunication engineering and Ph.D. degree in  
 7 Photonic from the University of Malaya, Malaysia in 2011 and 2015, respectively.  
 8 Currently, he is working as a post-doctoral fellow under Department of Electrical  
 9 Engineering, University of Malaya. His current research interests include sensor and  
 10 pulse fiber laser.

11 28.



12 29.

13 30. **Sayidal El Fatimah Masnan** received a B.Eng in Environmental Engineering from  
 14 University of Malaya in 2012. Currently, she is pursuing her master study in the  
 15 Department of Civil Engineering, University of Malaya.

16 31.

17 32.



18 33.

19 34.

20 35. **Norshazmira Mat Azmi** received a B.Eng in Environmental Engineering from  
 21 University of Malaya in 2012. Currently, she is pursuing her master study in the  
 22 Department of Civil Engineering, University of Malaya.

23 36.

24 37.

25 38.



39.

40.

41. **Shatirah Akib** received her M.Sc. in Civil Engineering from University of Wales, Cardiff, United Kingdom, in 2003 and her Ph.D. in Hydraulic Structure Engineering from University of Malaya, Malaysia in 2009. Currently, she is an Associate Professor at the School of Energy, Geoscience, Infrastructure and Society (EGIS), Heriot-Watt University, Putrajaya, Malaysia. Her current research areas are Hydraulics, Hydraulic Structure Engineering, Coastal and Offshore Engineering, Hydropower and Water Resources Engineering.

42.



43.

44.

45. **Hamzah Arof** received his Ph.D. degree from University of Swansea (UK) and he is currently a full Professor in the Department of Electrical Engineering, University of Malaya.



46.

47.

48. **Sulaiman Wadi Harun** received the B.E. degree in electrical and electronics system engineering from Nagaoka University of Technology, Japan in 1996, and M.Sc. and Ph.D. degrees in photonics from University of Malaya in 2001 and 2004, respectively. Currently, he is a full professor at the Faculty of Engineering, University of Malaya. His research interests include fiber optic active and passive devices.

49.

50.